JOURNAL OF SOLID STATE CHEMISTRY **128,** 150–155 (1997)
ARTICLE NO. SC967201

A New Structure Related to the Layered Cuprates: The "1201" Shear-Like Phase $Tl_5Ba_3Sr_5Cu_3O_{19}$, Third Member of the Series $(TlA_2CuO_5)_m \cdot Tl_2A_2O_4$

F. Letouzé, C. Martin, M. Hervieu, C. Michel, A. Maignan, and B. Raveau

Laboratoire CRISMAT, URA CNRS 1318, ISMRA, Bd du Maréchal Juin, 14050 Caen Cedex, France

Received June 4, 1996; in revised form October 18, 1996; accepted October 22, 1996

A thallium cuprate, $Tl_5Ba_3Sr_5Cu_3O_{19}$, whose structure can be derived by systematically shearing the "1201" structure has been synthesized for the first time. It crystallizes in an orthorhombic cell with $a = 3.7536(2)$ Å, $b = 30.631(2)$ Å, $c = 9.219(1)$ Å, and A-type symmetry. This new structure consists of "1201" ribbons parallel to (010) which are three CuO_6 octahedra wide and are interconnected through "$Tl_2A_2O_4$" ribbons whose cationic configuration is that of the rock salt structure. This phase can be considered to be the $m = 3$ member of a new series with the generic formulation $(TlA_2CuO_5)_m \cdot Tl_2A_2O_4$ with $A = Ba, Sr$.

© 1997 Academic Press

INTRODUCTION

The application of shearing mechanisms to the superconducting layered cuprates and oxycarbonates, transverse to the copper layers, has allowed several series of original structures to be generated. This is the case of some of the copper oxycarbonates involving thallium or mercury (1, 2). The thallium based compounds derive from the superconductor $Tl_{0.5}Pb_{0.5}Sr_4Cu_2(CO_3)O_7$ (3) an intergrowth of the "1201" $Tl_{0.5}Pb_{0.5}Sr_2CuO_5$ and $Sr_2Cu(CO_3)O_2$ (S_2CC) phases, obtained by a single shear. Through the shear plane, the copper layers are not interrupted allowing superconducting properties to be retained.

Besides these true shear structures, other series of phases have been synthesized by applying similar shearing mechanisms to the bismuth cuprates and oxycarbonates. In this way, collapsed bismuth phases, derived from the superconductors $Bi_2Sr_2CuO_6$, $Bi_2Sr_2CaCu_2O_8$, and $Bi_2Sr_4Cu_2(CO_3)O_8$, have been synthesized (4–6). These compounds are generated by the periodic formation of shear planes transverse to the copper layers every m octahedra with respect to the mother structure. They differ from the Tl or Hg based oxycarbonates by the fact that the copper layers are interrupted resulting in the loss of superconductivity. Moreover, the composition at the junction between two identical shifted blocks is different from the matrix, forming a thin layer a few angströms thick, with a structure different from that of the mother phase. Consequently, these phases are not considered to be true shear structures and for this reason are called "collapsed" or shear-like phases.

The strategy for the discovery of these new structures is based on very slight variations of compositions with respect to the mother structure, especially with the introduction of copper deficiency with respect to other cations. It can also be achieved with the variation of the Ba/Sr ratio. Curiously, no such collapsed structures derived from the thallium cuprates have been obtained to date. For this reason we have investigated the system Tl–Ba–Sr–Cu–O, around the composition $Tl(Ba, Sr)_2CuO_5$ (7), introducing a significant copper deficiency. We report herein on a new cuprate $Tl_5Ba_3Sr_5Cu_3O_{19}$ with an original structure, derived from the "1201" structure by a shearing mechanism.

EXPERIMENTAL

The samples were prepared by solid state reaction starting from the nominal 1201 composition according to the formulation $Tl_{1+x}Ba_{2-y}Sr_yCu_{1-x}O_{5-\delta}$, with x varying from 0 to 0.5 and y from 1 to 1.75. The starting oxides were Tl_2O_3, BaO_2 and $SrCuO_2$. BaO_2 was chosen in order to avoid the presence of carbonates. Mixtures were ground, pressed in the form of bars, and introduced in alumina crucibles. They were then placed in evacuated silica ampoules together with a second crucible where 1/4 Ti (in mole per 1201 unit) had been introduced in order to decrease the oxygen partial pressure. Different thermal processes were tried. The best results were obtained for the following thermal treatment. The temperature was ramped up to 880°C in 6 h, maintained for 6 h, and decreased down to room temperature by furnace cooling.

The powder X-ray diffraction study (XRD) was performed with a Philips diffractometer (Cu$K\alpha$ radiation) by step scanning over an angular range $6° \leq 2\theta \leq 95°$ with an

0022-4596/97 $25.00
Copyright © 1997 by Academic Press
All rights of reproduction in any form reserved.

increment of 0.02°. It was systematically coupled with EDS analyses using Kevex analyzers mounted on the transmission electron microscopes, operating at 200 KV.

The electron diffraction (ED) study was carried out with a JEOL 200 CX electron microscope, fitted with an eucentric goniometer ($\pm 60°$). The high resolution electron microscopy (HREM) study was performed with a TOPCON 002B microscope, having a point resolution of 1.8 Å. The samples were prepared by a smooth crushing of the crystals which were then deposited on a holey carbon film (Ni grid). Image calculations were performed using the Mac Tempas program.

RESULTS AND DISCUSSION

For the compositions close to $x = 0.25$ and $y = 1.25$, a new phase is obtained. The electron diffraction study shows that it exhibits an orthorhombic cell with $a \approx a_p$, $b \approx 8a_p \approx 30.6$ Å, and $c \approx c_{1201} \approx 9.2$ Å (a_p being the cell parameter of the ideal cubic perovskite). The conditions limiting the reflection are hkl: $k + l = 2n$, involving $A222$, $Am2m$, $Ammm$, and $A2mm$ as possible space groups. The [100] and [001] ED patterns are given in Figs. 1a and 1b, respectively.

The cell parameters have been refined from XRD data to $a = 3.7536$ (2) Å, $b = 30.631$ (2) Å, and $c = 9.219$ (1) Å.

The EDS analyses performed over numerous grains provided the actual cationic composition $Tl_5Ba_3Sr_5Cu_3$ which is in agreement with the nominal formula. The close geometrical relationships of the new compound cell parameters with those of the 1201-type phases ($a_p \times a_p \times 9.2$ Å) suggested that the two structures are directly related.

HREM and XRD Structure Investigation

The HREM study of the new phase was carried out, selecting the [100] orientation which would be theoretically the best for displaying information on the nature of the superstructure occurring along [010]. In a first step, the image interpretation was carried out considering the contrast usually observed in the 1201-type phases. Image simulations were then calculated from the positional parameters refined from XRD data (Table 1).

The HREM images where only the copper positions are highlighted are of interest since they provide an initial idea of the structure. An example of such an overall image is given in Fig. 2a. Along **b**, the periodicity over a distance of 8×3.8 Å can be simply described by the sequence of three bright dots (indicated by three adjacent white triangles) and five dark dots, involving three adjacent copper atoms separated by five different atoms. Similar layers, 4.65 Å spaced along **c**, are observed but systematically translated by $1/2\mathbf{b} + 1/2\mathbf{c}$, in agreement with the A-type symmetry of the cell.

Other important information is obtained from the [100] HREM images where the cation positions are imaged as bright dots. An example is given in Fig. 3. For a focus value, Δf, which is assumed to be close to -550 Å and a small crystal thickness ($t \approx 25$ Å) one observes bands parallel to (010) and that are three octahedra thick, running along **c** and whose contrast is similar to that usually observed along $\mathbf{c}_{1201}$ in the "1201" cuprates $TlBa_2CuO_5$: three adjacent infinite rows of staggered bright dots correlated to the $[BaO]_\infty$, $[TlO]_\infty$, and $[BaO]_\infty$ layers alternate with single rows of small grey dots, corresponding to the copper layers. Since the 1201 cell is tetragonal with $a = a_p$, the periodicity along $\mathbf{b}_{1201}$ is ≈ 3.8 Å. In our compound, the periodicity of the contrast along b is ≈ 30.6 Å, i.e., 8×3.8 Å, and two successive (010) 1201-type ribbons are shifted by $c/2$ with respect to each other (Fig. 3). Moreover between two "1201" ribbons that are three copper octahedra wide one observes three rows of staggered bright dots running along **c**, correlated to heavy cations whose arrangement is similar to that encountered in rock salt layers (Fig. 3). From these observations it appears that the five different atoms that alternate

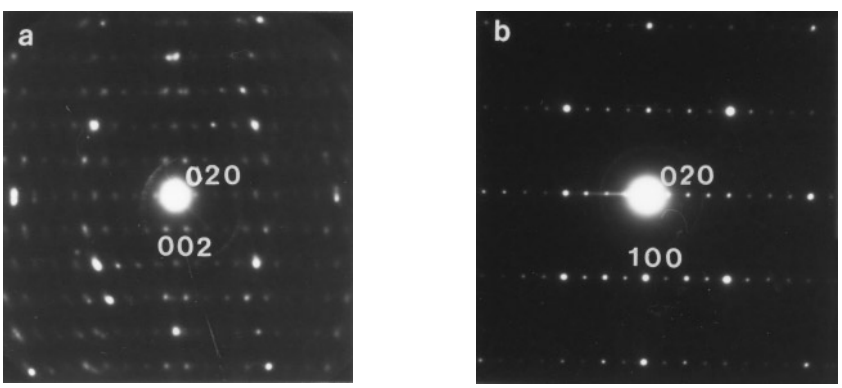

FIG. 1. $Tl_5Ba_3Sr_5Cu_3O_{19}$ (a) [100] and (b) [001] electron diffraction patterns.

TABLE 1
Initial and Refined Structural Parameters in the Space Group *A2mm* for $Tl_5Ba_3Sr_5Cu_3O_{19}$

		Initial parameters			Refined parameters			
Atom	Site	*x*	*y*	*z*	*x*	*y*	*z*	$B(Å^2)$
Tl(1)	2*b*	0.0	0.0	0.5	0.0	0.0	0.5	1.9(3)
Tl(2)	4*d*	0.0	0.125	0.5	0.0	0.1128(3)	0.5	2.3(3)
Tl(3)	4*d*	0.0	0.25	0.5	0.0	0.2397(3)	0.5	0.9(2)
Ba/Sr(1)	8*f*	0.5	0.0625	0.25	0.5	0.0615(4)	0.2011(7)	0.1(1)[c]
Ba/Sr(2)	8*f*	0.5	0.1875	0.25	0.5	0.1844(3)	0.2152(9)	0.1(1)[c]
Cu(1)	2*a*	0.0	0.0	0.0	0.0	0.0	0.0	1.6(7)
Cu(2)	4*d*	0.0	0.125	0.0	0.0	0.1212(7)[a]	0.0	1.3(6)
O(1)	2*a*	0.5	0.0	0.0	0.5	0.0	0.0	1.0
O(2)	4*d*	0.5	0.125	0.0	0.5	0.1212(7)[a]	0.0	1.0
O(3)	4*e*	0.0	0.0	0.25	0.0	0.0	0.263(2)[b]	1.0
O(4)	8*f*	0.0	0.125	0.25	0.0	0.1212(7)[a]	0.263(2)[b]	1.0
O(5)	4*d*	0.0	0.0625	0.0	0.0	0.0606(7)	0.0	1.0
O(6)	4*d*	0.5	0.0625	0.5	0.5	0.056(3)	0.5	1.0
O(7)	4*d*	0.5	0.1875	0.5	0.5	0.176(3)	0.5	1.0
O(8)	4*c*	0.0	0.25	0.25	0.0	0.25	0.25	1.0
O(9)	4*d*	0.0	0.1875	0.0	0.0	0.186(2)	0.0	1.0

Note. $a = 3.7536(2)$ Å, $b = 30.631(2)$ Å, and $c = 9.219(1)$ Å. $R_p = 9.67\%$, $R_{wp} = 12.9\%$, and $R_i = 9.13\%$. The Ba and Sr contents in the Ba/Sr(1) and Ba/Sr(2) sites were refined to 2.2(2) Ba + 5.8(2) Sr and 3.8(2) Ba + 4.2(2) Sr, respectively.
[a,b,c] Parameters constrained at the same value (see text).

with the three copper octahedra along **b** (Fig. 2) can be identified as thallium atoms.

On the basis of these HREM observations, which imply that two successive (010) "1201" ribbons correspond to each other though an *A*-type symmetry, an ideal model could be elaborated (Fig. 4) corresponding to the initial parameters given in Table 1. In order to check this hypothesis a Rietveld refinement on 328 *hkl* of the powder X-ray diffraction data was performed using the program FULLPROF (8) in the space group *A2mm*. Considering the large number of

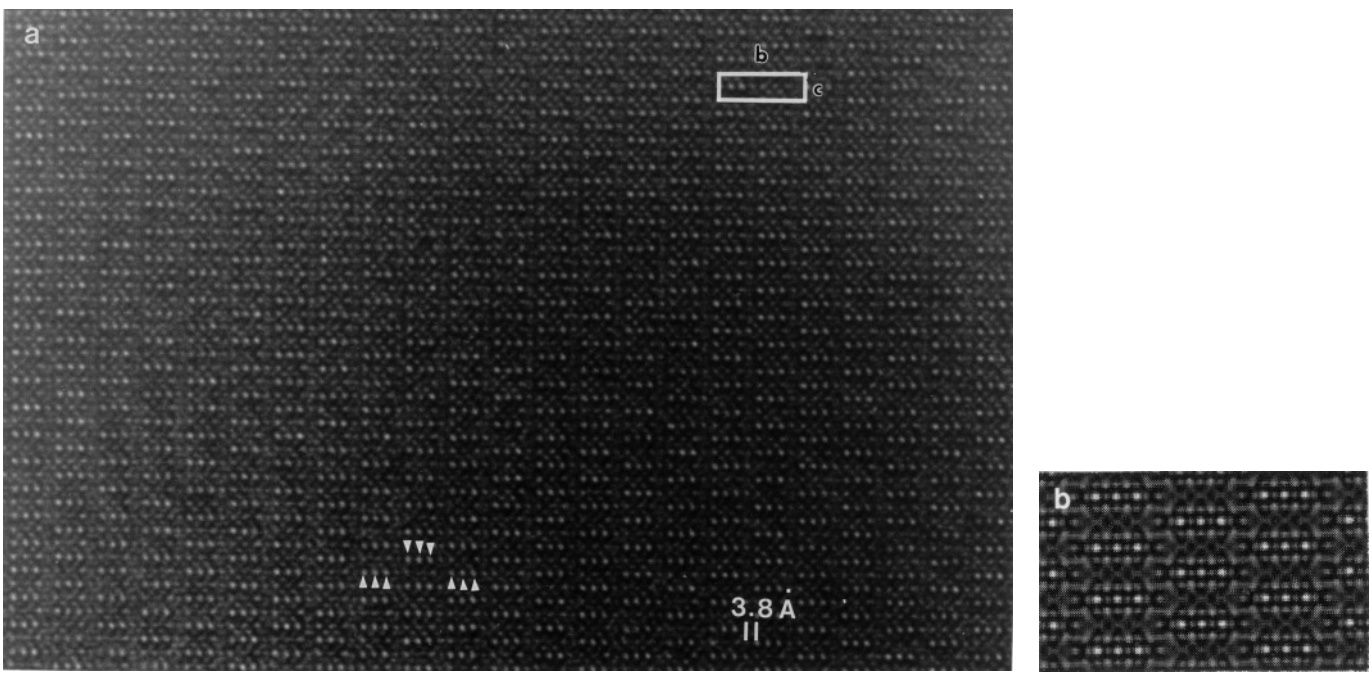

FIG. 2. $Tl_5Ba_3Sr_5Cu_3O_{19}$ (a) [100] HREM image where only the copper positions are highlighted (white triangles). The cell is outlined. Along **b**, three bright dots alternate with five grey dots; this sequence is shifted by $b/2$ in the adjacent layer. (b) Simulated image. The positional parameters are given in Table 1. The focus value is ≈ -450 Å and the crystal thickness is ≈ 60 Å.

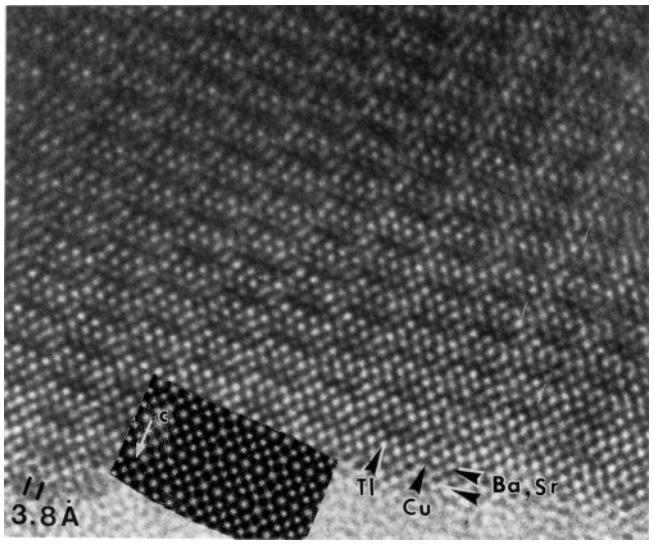

FIG. 3. [100] HREM where the cation positions appear as bright dots (identified in the right bottom part of the image). The calculated image ($\Delta \approx -550$ Å and $t \approx 25$ Å) is superimposed to the experimental one, on the crystal edge.

variable parameters, some of them were constrained during the refinements, especially those concerning oxygen atoms:

— O(2) and O(4) which belong to the Cu(2) octahedra (O(2) in the basal plane and O(4) as the apical oxygens) were constrained to have the same y parameter;

— O(3) and O(4) which are the apical oxygens of the Cu(1) and Cu(2) octahedra respectively were constrained to have the same z parameter;

— O(5) which connects Cu(1) to Cu(2) was constrained to have its y parameter equal to $1/2y_{Cu(2)}$.

Barium and strontium were first assumed to be randomly distributed over the two crystallographic sites; isotropic thermal factors for oxygens were fixed at 1 $Å^2$. Traces of $BaCO_3$ and Sr_2CuO_3, detected on the X-ray diffraction pattern, were introduced as secondary phases in the calculations.

Positional parameters for thallium ($y_{Tl(2)}$ and $y_{Tl(3)}$), barium and strontium (y and z), and copper ($y_{Cu(2)}$) were first refined, then those of the oxygens and the B factors for metallic atoms. Last, a possible ordering of barium and strontium between the two available sites was considered. The refined structural parameters are listed in Table 1. The corresponding agreements factors $R_p = 0.097$, $R_{wp} = 0.129$, and $R_i = 0.091$ attest of the validity of the model. The experimental, calculated and difference XRD patterns are plotted in Fig. 5.

These refined positional parameters were then used to simulate the [010] HREM images. The calculated through focus series fit perfectly with the experimental ones. The

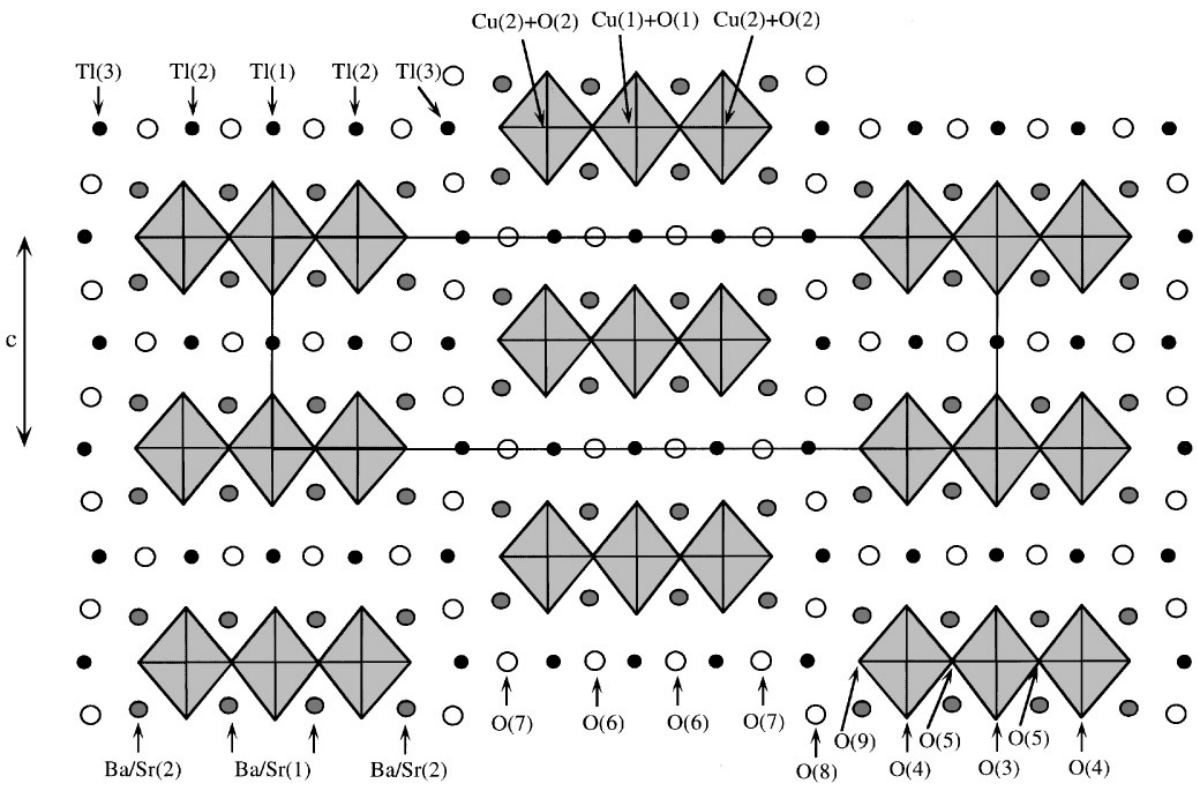

FIG. 4. Projection onto (100) of the structure of $Tl_5Ba_3Sr_5Cu_3O_{19}$. The different atoms are labeled.

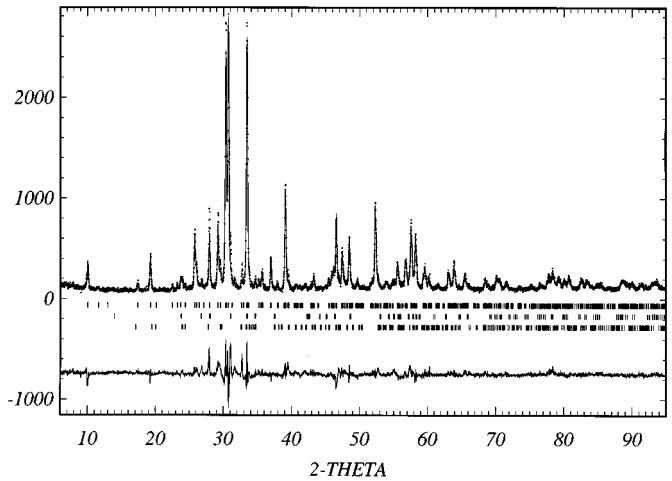

FIG. 5. X-ray diffraction patterns (experimental, dotted line; calculated, continuous line; and difference, bottom). The expected positions of the Bragg angles are indicated for the title compound and the impurities (Sr_2CuO_3 and $BaCO_3$).

calculated images corresponding to $\Delta f = -450$ Å/$t \approx 60$ Å and $\Delta f = -550$ Å/$t \approx 25$ Å are compared to the experimental images in Figs. 2b and 3, respectively.

Structural Model

From this study, a structural model is established that shows very close relationships between the cuprate $Tl_5Ba_3Sr_5Cu_3O_{19}$ and the "1201" structure of $TlBa_2CuO_5$. As shown from the projection of the structure onto the (100) plane (Fig. 4), this new cuprate consists of "1201" ribbons, parallel to (010) that are three CuO_6 octahedra wide; two successive ribbons are shifted by $c/2$, so that this phase can be considered as a shear like structure with respect to the "1201" structure. The important difference with the true shear structures deals with the fact that two successive "1201" ribbons are interconnected through a (010) thallium layer, whose atomic arrangement with the two surrounding barium (and strontium) layers exhibits a rock salt cationic configuration. As a consequence this new cuprate can be described as the $m = 3$ member of a large structural family with the generic formula $(TlA_2CuO_5)_m \cdot Tl_2A_2O_4$ with $A = Ba, Sr$.

An interesting characteristic of this structure deals with the fact that one observes mixed copper–thallium layers parallel to (001) built up of three copper rows and five thallium rows alternately, that are absolutely flat (Fig. 4). In contrast, the mixed barium–strontium layers are waving, due to the fact that in the "1201" structure the Sr/Ba layers are closer to the copper layers than to the thallium layers. Note also that barium and strontium are not really distributed at random over the two kinds of sites. Within the "1201" ribbons, the Ba/Sr(1) sites are mainly occupied by strontium (78%) whereas at the junction between two "1201" ribbons, i.e., in the $A_2Tl_2O_4$ ribbons, the Ba/Sr(2) sites are almost randomly occupied (48% strontium).

The Ba/Sr–O interatomic distances (Table 2), shorter for the Ba/Sr(1) site (mean value 2.67 Å) than for the Ba/Sr(2) site (mean value 2.73 Å), are in agreement with the refinement of the occupancy factors. The CuO_6 octahedra are characterized by four short in plane distances and two long apical distances. This is a common feature in cuprates involving perovskite monolayers. Tl(1) and Tl(2) forming the "1201" ribbons are sixfold coordinated with two short apical distances (2.18–2.20 Å) and four long in-plane distances (2.55–2.69 Å). These distances are close to those usually observed in the thallium cuprates. However it is seen from neutron diffraction studies that in the thallium cuprates involving thallium–oxygen monolayers, thallium and oxygens in the $[TlO]_\infty$ layers are split over more general positions leading to a thallium environment better described as a tetrahedron than a distorted octahedron. This was not tested in the present study considering the great number of variable parameters but the relatively high B values obtained for Tl(1) and Tl(2) could be the sign of such splitting. The Tl(3) atoms that form the $[Tl_2A_2O_4]_\infty$ ribbons parallel to (010) exhibit an unusual bipyramidal trigonal coordination, but the lack of accuracy about the determination of the oxygen positions in those ribbons suggests that the atomic arrangement in such ribbons is more complex. Nevertheless Fourier difference maps at the level of Tl(3) after removing the neighboring oxygens did not allow the proposal of alternate environments. The problem of the exact nature of the thallium–oxygen polyhedra forming the junction between two 1201 blocks appears to be similar to that encountered in the case of the 2201 collapsed bismuth cuprates (5) and will require neutron diffraction data to resolve.

TABLE 2
Interatomic Bond Distances

M–O	Distance (Å)	*x n*	*M*–O	Distance (Å)	*x n*
Tl(1)–O(3)	2.18(2)	2	Ba/Sr(1)–O(1)	2.64(1)	1
–O(6)	2.55(5)	4	–O(2)	2.60(2)	1
Tl(2)–O(4)	2.20(2)	2	–O(3)	2.72(1)	2
–O(6)	2.55(6)	2	–O(4)	2.68(2)	2
–O(7)	2.69(6)	2	–O(5)	2.64(1)	2
Tl(3)–O(7)	2.71(6)	2	–O(6)	2.76(1)	1
–O(8)	2.33(1)	2	Ba/Sr(2)–O(2)	2.77(2)	1
–O(9)	2.27(8)	1	–O(4)	2.73(2)	2
Cu(1)–O(1)	1.877(1)	2	–O(7)	2.64(1)	1
–O(3)	2.42(2)	2	–O(8)	2.77(1)	2
–O(5)	1.86(2)	2	–O(9)	2.73(1)	2
Cu(2)–O(2)	1.877(1)	2			
–O(4)	2.42(2)	2			
–O(5)	1.86(3)	1			
–O(9)	1.99(8)	1			

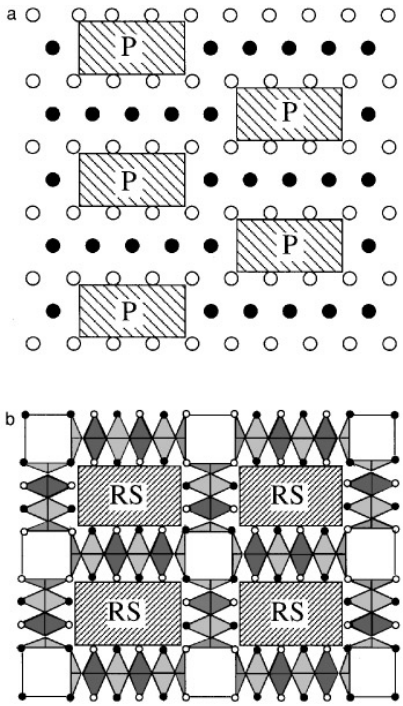

FIG. 6. Idealized drawing of the (a) $Tl_5Ba_3Sr_5Cu_3O_{19}$ structure: the member $m = 3$ of the antitubular 1201 structure. The rock salt framework forming the tubes are filled up by perovskite units. (b) $Bi_4Sr_8Cu_5O_{19}$ structure: the member $m = 4$ of the tubular 2201 bismuth structure. The perovskite framework forming the tubes are filled up by rock salt units.

Finally, one remarkable feature of this structure deals with the arrangement of the Tl, Ba, and Sr atoms that form a tridimensional cationic network in which the cations exhibit the positions occupied in a rock salt structure and form rectangular tubes running along **a** (Fig. 6a). In such a tubular structure, the tunnels are filled with triple rows of copper octahedra. Such a tridimensional framework exhibits similarity with the "2201" tubular structure of the cuprate $Bi_4Sr_8Cu_5O_{19}$ (9, 10) (Fig. 6b) whose host lattice consists of cross linked perovskite layers also forming rectangular tunnels. In the latter, the tunnels are filled with triple rock salt ribbons. In other words, the structure of $Tl_5Ba_3Sr_5Cu_3O_{19}$ can be considered as an anti-"1201" tubular structure.

CONCLUDING REMARKS

The possibility to generate a new structure type by a shearing mechanism in a thallium cuprate is shown for the first time. This study opens the route to the exploration of a new series of thallium cuprates with the formula $(TlA_2CuO_5)_m \cdot A_2Tl_2O_4$, closely related to the "1201" type cuprates.

The existence of mixed thallium–copper layers characterized by a strict ordering of thallium and copper is a remarkable characteristic of this new phase, and has not previously been observed in thallium cuprates. The analogy of this structure with the tubular bismuth cuprate is another interesting feature. The existence of a bidimensional cationic network with the rock salt configuration suggests that other structures with various sizes of the tunnels may exist.

Finally it is worth pointing out that this new phase is insulating in spite of the fact that its chemical formula implies the presence of holes in the copper–oxygen polyhedra. Such behavior may be related to the fact that there are no infinite copper–oxygen planes but only narrow ribbons.

The issue of oxygen nonstoichiometry in this phase, especially with respect to the coordination of thallium in the transverse $Tl_2A_2O_4$ layers is not yet elucidated. A neutron diffraction study will be necessary to understand this behavior.

REFERENCES

1. F. Goutenoire, M. Hervieu, A. Maignan, C. Michel, C. Martin, and B. Raveau, *Physica C* **210,** 359 (1993).
2. A. Maignan, D. Pelloquin, S. Malo, C. Michel, M. Hervieu, and B. Raveau, *Physica C* **249,** 220 (1995).
3. M. Huvé, C. Michel, A. Maignan, M. Hervieu, C. Martin, and B. Raveau, *Physica C* **205,** 219 (1993).
4. M. Hervieu, C. Michel, A. Q. Pham, and B. Raveau, *J. Solid State Chem.* **104,** 338 (1993).
5. M. Hervieu, M. T. Caldès, S. Cabrera, C. Michel, D. Pelloquin, and B. Raveau, *J. Solid State Chem.* **119,** 169 (1995).
6. M. Hervieu, M. T. Caldès, D. Pelloquin, C. Michel, S. Cabrera, and B. Raveau, *J. Mater. Chem.* **6,** 175 (1996).
7. I. K. Gopalakrishnan, J. V. Yakhmi, and R. M. Iyer, *Physica C* **175,** 183 (1991).
8. J. Rodriguez-Carvajal, *in* "Collected Abstracts of Powder Diffraction Meeting" (J. Galy, Ed.), p. 127. Toulouse, 1990.
9. A. Fuertès, C. Miravitlles, J. Gonzalez-Calbet, M. Vallet-Regi, X. Obradors, and J. Rodriguez-Carvajal, *Physica C* **157,** 525 (1989).
10. M. T. Caldès, M. Hervieu, A. Fuertès, and B. Raveau, *J. Solid State Chem.* **97,** 48 (1992).